Inorg. Chem. **2006**, *45*, 5034–5043

Novel Biscapped and Monocapped Tris(dioxime) Mn(II) Complexes: X-ray Crystal Structure of the First Cationic Tris(dioxime) Mn(II) Complex $[Mn(CDOH)_3BPh]OH$ ($CDOH_2$ = 1,2-cyclohexanedione dioxime)

Wen-Yuan Hsieh and Shuang Liu*

Department of Industrial & Physical Pharmacy, School of Health Sciences, Purdue University, 550 Stadium Mall Drive, West Lafayette, Indiana 47907

Received February 7, 2006

This report describes the synthesis and characterization of a series of novel biscapped and monocapped tris(dioxime) Mn(II) complexes $[Mn(dioxime)_3(BR)_2]$ and $[Mn(dioxime)_3BR]^+$ (dioxime = cyclohexanedione dioxime ($CDOH_2$) and 1,2-dimethylglyoxyl dioxime ($DMGH_2$); R = Me, *n*-Bu, and Ph). All tris(dioxime) Mn(II) complexes have been characterized by elemental analysis, IR, UV/vis, cyclic voltammetry, ESI-MS, and, in the cases of $[Mn(CDOH)_3BPh]OH{\cdot}CHCl_3$ and $[Mn(CDO)(CDOH)_2(BBu(OC_2H_5))_2]$, X-ray crystallography. It was found that biscapped Mn(II) complexes $[Mn(dioxime)_3(BR)_2]$ are not stable in the presence of water and readily hydrolyze to form monocapped cationic complexes $[M(dioxime)_3BR]^+$. This instability is most likely caused by mismatch between the size of Mn(II) and the coordination cavity of the biscapped tris(dioxime) ligands. In contrast, monocapped cationic complexes $[M(dioxime)_3BR]^+$ are very stable in aqueous solution even in the presence of PDTA (1,2-diaminopropane-*N*,*N*,*N*′,*N*′-tetraacetic acid) because of the kinetic inertness imposed by the monocapped tris(dioxime) chelators that are able to completely "wrap" Mn(II) into their N_6 coordination cavity. $[Mn(CDO)_3BPh]OH$ has a distorted trigonal prismatic coordination geometry, with the Mn(II) being bonded by six imine-N donors. The hydroxyl groups from three dioxime chelating arms form very strong intramolecular hydrogen bonds with the hydroxide counterion so that the structure of $[Mn(CDOH)_3BPh]OH$ can be considered as being the clathrochelate with the hydroxide counterion as a "cap".

Introduction

There is a burgeoning interest in Mn(II) complexes as magnetic resonance imaging (MRI) contrast agents.[1−5] For Mn(II) complexes to be useful as MRI contrast agents, they must have a sufficient solution stability to withstand transchelation in the blood circulation. However, most Mn(II) complexes have a low solution stability, because of the d^5 configuration of Mn(II) and a lack of ligand-field stabilization energy. The thermodynamic stability of Mn(II) complexes can be improved by using chelators, such as EDTA (ethylenediaminetetraacetic acid) and DTPA (diethylenetriaminepentaacetic acid);[6] but they often undergo rapid ligand exchange because of their lack of kinetic inertness. This may explain why thermodynamically stable Mn(II) complexes, such as Mn-DPDP (DPDP = *N*,*N*′-dipyridoxylethylenediamine-*N*,*N*-diacetate-5,5-bis(phosphonate)), decompose rapidly to produce the "free" Mn(II) ions once they are injected into the biological system.[7−10] Despite the success of Mn-

* To whom correspondence should be addressed. Address: Room 1275, Civil Engineering Building, School of Health Sciences, Purdue University, 550 Stadium Mall Drive, West Lafayette, IN 47907. Phone: 765-494-0236. Fax 765-496-1377. E-mail: lius@pharmacy.purdue.edu.

(1) Lauffer, R. B. *Chem. Rev.* **1987**, *87*, 901−927.
(2) Storey, P.; Danias, P. G.; Post, M.; Li, W.; Seoane, P. R.; Harnish, P. P.; Edelman, R. R.; Prasad, P. V. *Invest. Radiol.* **2003**, *38*, 642−652.
(3) Kruk, D.; Kowalewski, J. *J. Biol. Inorg. Chem.* **2003**, *8*, 512−518.
(4) Aime, S.; Anelli, P. L.; Botta, M.; Brocchetta, M.; Canton, S.; Fedeli, F.; Gianolio, E.; Terreno, E. *J. Biol. Inorg. Chem.* **2002**, *7*, 58−67.
(5) Troughton, J. S.; Greenfield, M. T.; Greenwood, J. M.; Dumas, S.; Wiethoff, A. J.; Wang, J.; Spiller, M.; McMurry, T. J.; Caravan, P. *Inorg. Chem.* **2004**, *43*, 6313−6323.
(6) Ogino, H. *Bull. Chem. Soc. Jpn.* **1965**, *38*, 771−778.
(7) Federle, M. P.; Chezmar, J. L.; Rubin, D. L.; Weinreb, J. C.; Freeny, P. C.; Schmiedl, U. P.; Brown, J. J.; Borrello, J. A.; Lee, J. K. T.; Semelka, R. C.; Mattrey, R.; Dachman, A. H.; Saini, S.; Harms, S. E.; Mitchell, D. G.; Anderson, M. W.; Halford, H. H., III; Bennett, W. F.; Young, S. W.; Rifkin, M.; Gay, S. B.; Ballerini, R.; Sherwin, P. F.; Robison, R. O. *J. Magn. Reson. Imaging* **2000**, *12*, 689−701.
(8) Gallez, B.; Baudelet, C.; Adline, J.; Geurts, M.; Delzenne, N. *Chem. Res. Toxicol.* **1997**, *10*, 360−363.
(9) Gallez, B.; Baudelet, C.; Geurts, M. *Magn. Reson. Imaging* **1998**, *16*, 1211−1215.
(10) Schmidt, P. P.; Toft, K. G.; Skotland, T.; Andersson, K. K. *J. Biol. Inorg. Chem.* **2002**, *7*, 241−248.

10.1021/ic060216n CCC: $33.50
Published on Web 05/25/2006

DPDP in the detection of liver and cardiovascular diseases,[11−13] there is a continuing need for Mn(II) complex contrast agents with improved solution stability.

One approach to achieving a high solution stability of Mn(II) complexes is to increase their kinetic inertness. For example, macrocyclic pentaamines, such as 1,4,7,10,13-pentaazacyclo-pentadecane, have been used to prepare Mn(II) complexes with a high solution stability, because these macrocycles are able to impart kinetic inertness by wrapping Mn(II) into their N_5 coordination cavity.[14−17] Mn(II) complexes of C-substituted macrocyclic pentaamines have been studied as manganese superoxide dismutase (Mn-SOD) mimetics that are useful for the treatment of diseases, such as myocardial ischemia reperfusion injury, inflammation, and cerebral ischemia injury.[18−23] Macrocyclic chelators, such as 1,4,7,10-tetraazacyclododecane-1,4,7,10-tetraacetic acid (DOTA) and 1,4,7,10-tetraazacyclododecane-1,4-diacetic acid (DO2A), have also been used to prepare Mn(II) complexes with high thermodynamic stability and kinetic inertness.[24,25]

In this report, we describe a new approach to achieving high solution stability for Mn(II) complexes by using the boron-capped tris(dioxime) chelators that are able to completely wrap the Mn(II) into their N_6 coordination cavity.

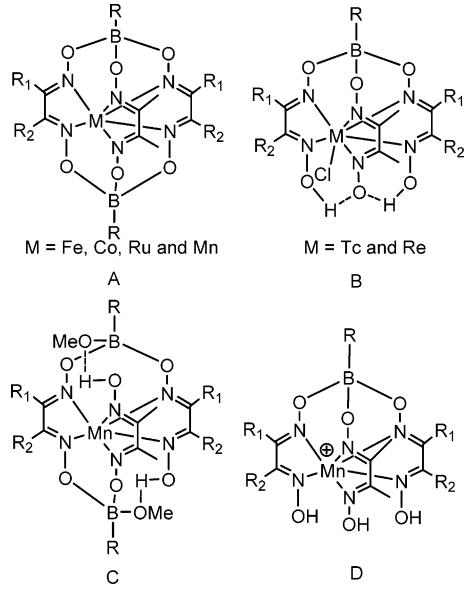

Figure 1. Mn(II) complexes with BATO type chelators, where R can be methyl or butyl phenyl groups.

We are particularly interested in cationic Mn(II) complexes, $[Mn(dioxime)_3BR]^+$ (Figure 1, complex D; dioxime = $CDOH_2$ (cyclohexanedione dioxime) and $DMGH_2$ (1,2-dimethylglyoxyl dioxime); R = Me, *n*-Bu, and Ph), because of their similarity to the Tc(III) complexes $[^{99m}TcCl(dioxime)_3BR]$ (Figure 1, complex B), which have been studied as potential radiotracers for myocardial perfusion imaging.[26−31] As a matter of fact, $[^{99m}TcCl(CDOH)_3BCH_3]$ is a radiopharmaceutical approved by the FDA (Food and Drug Administration) for heart imaging under the tradename of Cardiotec. It is postulated that like their ^{99m}Tc(III) analogues, cationic complexes $[Mn(dioxime)_3BR]^+$ might be able to selectively localize in the heart because of their cationic nature.

As the first step in our research toward new Mn(II)-based MRI contrast agents, we now present the synthesis and characterization of novel tris(dioxime) Mn(II) complexes (Figure 1, complexes A and D) as well as the X-ray crystal structure of the cationic complex $[Mn(CDOH)_3BPh]OH$. Different alkyl or aryl groups in dioxime chelating arms and boron caps were used to modify the lipophilicity and water solubility of the boron-capped tris(dioxime) Mn(II) complexes. The main objective is to determine their structures and study their stability in aqueous solution.

Tris(dioxime) metal complexes $[M(dioxime)_3(BR)_2]$ (Figure 1, complex A; M = Fe, Co, Ru) have been known for

(11) Federle, M. P.; Chezmar, J. L.; Rubin, D. L.; Weinreb, J. C.; Freeny, P. C.; Semelka, R. C.; Brown, J. J.; Borrello, J. A.; Lee, J. K. T.; Mattrey, R.; Dachman, A. H.; Saini, S.; Harmon, B.; Fenstermacher, M.; Pelsang, R. E.; Harms, S. E.; Mitchell, D. G.; Halford, H. H., III; Anderson, M. W.; Johnson, D.; Francis, I. R.; Bova, J. G.; Kenney, P. J.; Klippenstein, D. L.; Foster, G. S.; Turner, D. A.; Stillman, A. E.; Nelson, R. C.; Young, S. W.; Patt, R. H.; Rifkin, M.; Seltzer, S. E.; Gay, S. B.; Robison, R. O.; Sherwin, P. F.; Ballerini, R. *J. Magn. Reson. Imaging* **2000**, *12*, 186−197.

(12) Wyttenbach, R.; Saeed, M.; Wendland, M. F.; Geschwind, J.-F.; Bremerich, J.; Arheden, H.; Higgins, C. B. *J Magn. Reson. Imaging* **1999**, *9*, 209−214.

(13) Brurok, H.; Skoglund, T.; Berg, K.; Skarra, S.; Karlsson, J. O. G.; Jynge, P. *NMR Biomed.* **1999**, *12*, 364−372.

(14) Riley, D. P.; Henke, S. L.; Lennon, P. J.; Weiss, R. H.; Neumann, W. L.; Rivers, W. J.; Aston, K. W.; Sample, K. R.; Rahman, H.; Ling, C. S.; Shieh, J. J.; Busch, D. H.; Szulbinski, W. *Inorg. Chem.* **1996**, *35*, 5213−5231.

(15) Riley, D. P.; Lennon, P. J.; Neumann, W. L.; Weiss, R. H. *J. Am. Chem. Soc.* **1997**, *119*, 6522−6528.

(16) Riley, D. P.; Henke, S. L.; Lennon, P. J.; Aston, K. *Inorg. Chem.* **1996**, *35*, 1908−1917.

(17) Aston, K.; Rath, N.; Naik, A.; Slomczynska, U.; Schall, O. F.; Riley, D. P. *Inorg. Chem.* **2001**, *40*, 1779−1789.

(18) (a) Weiss, R. H.; Riley, D. P. *Drugs Future* **1996**, *21*, 383−389. (b) Riley, D. P. *Adv. Supramol. Chem.* **1999**, *6*, 217−244. (c) Riley, D. P. *Chem. Rev.* **1999**, *99*, 2573−2587. (d) Salvemini, D.; Muscoli, C.; Riley, D.; Cuzzocrea, S. *Pulm. Pharmacol. Ther.* **2002**, *15*, 439−447. (e) Salvemini, D.; Riley, D. P.; Cuzzocrea, S. *Nature Rev.* **2002**, *1*, 367−374.

(19) Salvemini, D.; Wang, Z.-Q.; Zweier, J. L.; Samouilov, A.; MacArthur, H.; Misko, T.; Currie, M. G.; Cuzzocreas, S.; Sikorski, J. A.; Riley, D. P. *Science* **1999**, *286*, 304−306.

(20) Weiss, R. H.; Fretland, D. J.; Baron, D. A.; Ryan, U. S.; Riley, D. P. *J. Biol. Chem.* **1996**, *271*, 26149−26156.

(21) Cuzzocrea, S.; Muzzon, E.; Dugo, L.; Caputi, A. P.; Aston, K.; Riley, D. P.; Salvemini, D. *Brit. J. Pharmacol.* **2001**, *132*, 19−29.

(22) Salvemini, D.; Mazzon, E.; Dugo, L.; Serraino, I.; De Sarro, A.; Caputi, A. P.; Cuzzocrea, S. *Arthritis Rheum.* **2001**, *44*, 2909−2921.

(23) Di Filippo, C.; Cuzzocrea, S.; Marfella, R.; Fabbroni, V.; Scollo, G.; Benino, L.; Giugliano, D.; Rossi, F.; D'Amico, M. *Eur. J. Pharmacol.* **2004**, *497*, 65−74.

(24) Chaves, S.; Delgado, R.; Frausto Da Silva, J. J. R. *Talanta* **1992**, *39*, 249−254.

(25) Bianchi, A.; Calabi, L.; Giorgi, C.; Losi, P.; Mariani, P.; Palano, D.; Paoli, P.; Rossi, P.; Valtancoli, B. *J. Chem. Soc., Dalton Trans.* **2001**, 917−922.

(26) Treher, E. N.; Francesconi, L. C.; Gougoutas, J. Z.; Malley, M. F.; Nunn, A. D. *Inorg. Chem.* **1989**, *28*, 3411−3416.

(27) Jurisson, S.; Halihan, M. M.; Lydon, J. D.; Barnes, C. L.; Nowotnik, D. P.; Nunn, A. D. *Inorg. Chem.* **1998**, *37*, 1922−1928.

(28) Linder, K. E.; Malley, M. F.; Gougoutas, J. Z.; Unger, S. E.; Nunn, A. D. *Inorg. Chem.* **1990**, *29*, 2428−2434.

(29) Jurisson, S.; Francesconi, L.; Linder, K. E.; Treher, E.; Malley, M. F.; Gougoutas, J. Z.; Nunn, A. D. *Inorg. Chem.* **1991**, *30*, 1820−1827.

(30) Narra, R. K.; Nunn, A. D.; Kuczynski, B. L.; Feld, T.; Wedeking, P.; Eckelman, W. C. *J. Nucl. Med.* **1989**, *30*, 1830−1837.

(31) Narra, R. K.; Nunn, A. D.; Kuczynski, B. L.; Di Rocco, R. J.; Feld, T.; Silva, D. A.; Eckelman, W. C. *J. Nucl. Med.* **1990**, *31*, 1370−1377.

many years.[32−39] However, very limited information is available on Mn(II) complexes [Mn(dioxime)$_3$(BR)$_2$] (Figure 1, complex A; dioxime = $CDOH_2$ and $DMGH_2$; R = Me, *n*-Bu, and Ph). The structure of [Mn(CDO)(CDOH)$_2$(BPh(OCH$_3$))$_2$] has been reported by Jurisson and co-workers,[29] but it has an unusual biscapped structure (Figure 1, complex C), in which only two of the three dioxime oxygen atoms are covalently bonded to the capping boron atoms. The X-ray crystal structure of [Mn(CDOH)$_3$BPh]OH represents the first example of structurally characterized cationic Mn(II) complexes with boron-capped tris(dioxime) ligands.

Experimental Section

Materials and Methods. All chemicals were purchased from Sigma Aldrich (St. Louis, MO) and used without purification. Infrared (IR) spectra (4000−400 cm^{-1}) were recorded on a Perkin−Elmer FT-IR spectrometer. UV/visible spectra were recorded on a Beckman DU-640 UV/vis spectrometer. Electrospray ionization mass spectral (ESI-MS) data were collected on a Finnigan LCQ classic mass spectrometer at the School of Pharmacy, Purdue University. Elemental analysis was performed with a Perkin−Elmer Series III analyzer at the Department of Chemistry, Purdue University. The HPLC method used a LabAlliance semi-prep HPLC system with a LabAlliance UV/vis detector (λ = 265 nm) and a Zorbax Rx-C18 column (4.6 × 150 mm, 5 μm). The flow rate was 1 mL/min, with the mobile phase starting from 100% solvent A (10 mM NH_4OAc buffer, pH 6.8) and changing to 90% solvent A and 10% solvent B (acetonitrile) at 10 min and 50% solvent A and 50% solvent B at 20 min. Cyclic voltammograms of Mn(II) complexes were recorded on a Bioanalytical System BAS-100A electrochemical analyzer. A standard three-electrode cell was used with a polished glassy-carbon working electrode, a Pt wire as the auxiliary electrode, and $Ag/AgNO_3$ in acetonitrile solution as the reference electrode. All measurements were performed in acetonitrile containing 0.1 M *n*-Bu_4NPF_6 at a scan rate of 100 mV/s. The sample solution was blanketed with extra pure N_2 gas during the experiment.

General Procedure for Preparation of Biscapped [Mn(dioxime)$_3$(BR)$_2$]. To a solution containing anhydrous $MnCl_2$ (0.255 g, 2 mmol) in 30 mL of absolute ethanol was added the dioxime (6 mmol) in 30 mL of ethanol under a nitrogen atmosphere. After the solution was refluxed for 60 min, alkyl- or arylboronic acid (4 mmol) in 20 mL of degassed ethanol was added. The mixture was stirred at room temperature for 2 h. The light brown precipitate was filtered and dried under vacuum overnight. Recrystallization of the crude product in the appropriate solvent or solvent mixture afforded the pure product, which was dried under vacuum for 4 h at room temperature before being submitted for elemental analysis.

[Mn(CDO)$_3$(BPh)$_2$]. The compound was recrystallized from acetonitrile and chloroform (50:50 v/v). Yield: 1.05 g (76%). IR (KBr, cm^{-1}): 1605, 1513, 1453, 1419 (s, $\upsilon_{C=N}$ and υ_{ring}); 1211, 1043 (s, υ_{N-O}); 1172 and 810, (s, υ_{B-O}). ESI-MS *m*/*z*: (negative mode) 650 (calcd for $[MnC_{30}H_{33}N_6O_6B_2]^-$, 650.20); (positive mode) 566 (calcd for $[MnC_{24}H_{32}N_6O_6B]^+$, 650.20).

[Mn(CDO)(CDOH)$_2$(BBu(OC$_2$H$_5$))$_2$]. Crystals of [Mn(CDO)(CDOH)$_2$(BBu(OC$_2$H$_5$))$_2$] were obtained from evaporation of the ethanol containing [Mn(CDO)$_3$(BBu)$_2$]. Yield: 0.46 g (∼65%). IR (KBr, cm^{-1}): 3385 (s, υ_{O-H}); 1562, (s, $\upsilon_{C=N}$); 1211, 1057 (s, υ_{N-O}); 1172 and 810, (s, υ_{B-O}). ESI-MS *m*/*z*: (positive mode) 546 (calcd for $[MnC_{22}H_{36}N_6O_6B]^+$, 546.22).

[Mn(CDO)$_3$(BCH$_3$)$_2$]. The compound was recrystallized from a mixture of acetonitrile and chloroform (50:50 v/v). Yield: 0.41 g (66%). IR (KBr, cm^{-1}): 3434 (s, υ_{O-H}); 1513, (s, $\upsilon_{C=N}$); 1211, 1043, (s, υ_{N-O}); 1172 and 810 (s, υ_{B-O}). ESI-MS *m*/*z*: (positive mode) 504 (calcd for $[MnC_{19}H_{30}N_6O_6B]^+$, 504.23).

[Mn(DMG)$_3$(BPh)$_2$]. The compound was recrystallized from a mixture of acetonitrile and methanol (50:50 v/v). Yield: 0.38 g (66%). IR (KBr, cm^{-1}): 1605, 1513, 1453, 1419, 1340 (s, $\upsilon_{C=N}$ and υ_{ring}); 1201, 1043 (s, υ_{N-O}); 1172 and 810, (s, υ_{B-O}). ESI-MS *m*/*z*: (negative mode) 572 for $[MnC_{24}H_{27}N_6O_6B]^-$; (positive mode) 488 (calcd for $[MnC_{18}H_{27}N_6O_6B]^+$, 488.14).

[Mn(DMG)$_3$(BBu)$_2$]. The compound was recrystallized from a mixture of acetonitrile and methanol (50:50 v/v). Yield: 0.32 g (60%). IR (KBr, cm^{-1}): 3410 (s, υ_{O-H}); 1513 (s, $\upsilon_{C=N}$); 1201, 1043 (s, υ_{N-O}); 1172 and 810 (s, υ_{B-O}). ESI-MS *m*/*z*: (positive mode) 468 (calcd for $[MnC_{16}H_{29}N_6O_6B]^+$, 468.17).

[Mn(DMG)$_3$(BCH$_3$)$_2$]. The compound was recrystallized from a mixture of acetonitrile and methanol (50:50 v/v). Yield: 0.28 g (62%). IR (KBr, cm^{-1}): 3350 (s, υ_{O-H}); 1513 (s, $\upsilon_{C=N}$); 1201, 1043 (s, υ_{N-O}); 1172 and 810 (s, υ_{B-O}). ESI-MS *m*/*z*: (positive mode) 426 (calcd for $[MnC_{13}H_{23}N_6O_6B]^+$, 426.12).

General Procedure for Preparation of Monocapped [Mn(dioxime)$_3$BR]$^+$. $Mn(OAc)_2{\cdot}4H_2O$ (0.49 g, 2 mmol) and dioxime (6 mmol) were dissolved in 50 mL of degassed absolute ethanol under a nitrogen atmosphere. After the solution was refluxed for 3 h, alkyl or arylboronic acid (2 mmol) in 20 mL of degassed ethanol was added slowly in order to minimize formation of the corresponding biscapped Mn(II) complex. The mixture was refluxed for 2 h, and the volume was reduced to ∼10% to give a brown precipitate. The solid was filtered, washed with cold ethanol and diethyl ether, and dried under vacuum for 4 h at room temperature before being submitted for elemental analysis.

[Mn(CDOH)$_3$BPh]Cl. Yield: 0.65 g (68%). IR (KBr, cm^{-1}): 3401 (s, υ_{O-H}); 1636, 1605, 1562, 1445, 1421, 1340 (s, $\upsilon_{C=N}$ and υ_{ring}); 1211, 1057 (s, υ_{N-O}); 1172 and 810 (s, υ_{B-O}). ESI-MS *m*/*z*: (positive mode) 566 (calcd for $[MnC_{24}H_{32}N_6O_6B]^+$, 566.19).

[Mn(CDOH)$_3$BBu]Cl. Yield: 0.38 g (62%). IR (KBr, cm^{-1}): 3395 (s, υ_{O-H}); 1557 (s, $\upsilon_{C=N}$); 1211, 1057 (s, υ_{N-O}); 1172 and 810 (s, υ_{B-O}). ESI-MS *m*/*z*: (positive mode) 546 (calcd for $[MnC_{22}H_{36}N_6O_6B]^+$, 546.22).

[Mn(CDOH)$_3$BCH$_3$]Cl. Yield: 0.56 g (65%). IR (KBr, cm^{-1}): 3144 (s, υ_{O-H}); 1552 (s, $\upsilon_{C=N}$); 1211, 1043 (s, υ_{N-O}); 1172 and 810 (s, υ_{B-O}). ESI-MS *m*/*z*: (positive mode) 504 (calcd for $[MnC_{19}H_{30}N_6O_6B]^+$, 504.23).

[Mn(DMGH)$_3$BPh]OAc. Yield: 0.34 g (62%). IR (KBr, cm^{-1}): 3387 (s, υ_{O-H}); 1677 (s, $\upsilon_{C=O}$); 1605, 1513, 1453, 1419, 1340 (s, $\upsilon_{C=N}$ and υ_{ring}); 1201, 1043 (s, υ_{N-O}); 1172 and 810 (s, υ_{B-O}). ESI-MS *m*/*z*: (positive mode) 488 (calcd for $[MnC_{18}H_{27}N_6O_6B]^+$, 488.14).

[Mn(DMGH)$_3$BBu]OAc. Yield: 0.33 g (63%). IR (KBr, cm^{-1}): 3404 (s, υ_{O-H}); 1667, 1513 (s, $\upsilon_{C=O}$ and $\upsilon_{C=N}$); 1201, 1043 (s, υ_{N-O}); 1172 and 810 (s, υ_{B-O}). ESI-MS *m*/*z*: (positive mode) 468 (calcd for $[MnC_{16}H_{29}N_6O_6B]^+$, 468.17).

[Mn(DMGH)$_3$BCH$_3$]OAc. Yield: 0.31 g (64%). IR (KBr, cm^{-1}): 3405 (s, υ_{O-H}); 1675, 1510 (s, $\upsilon_{C=O}$ and $\upsilon_{C=N}$); 1201, 1043

(32) Busch, D. H. *Rec. Chem. Prog.* **1964**, *25*, 107−126.
(33) Jackels, S. C.; Dierdorf, D. S.; Rose, N. J. *J. Chem. Soc., Chem. Commun.* **1972**, 1291−1292.
(34) Boston, D. R.; Rose, N. J. *J. Am. Chem. Soc.* **1968**, *90*, 6859−6860.
(35) Boston, D. R.; Rose, N. J. *J. Am. Chem. Soc.* **1973**, *95*, 4163−4168.
(36) Johnson, J. N.; Rose, N. J. *Inorg. Synth.* **1982**, *21*, 112−114.
(37) Robbins, M. K.; Naser, D. W.; Heiland, J. L.; Grzybowski, J. J. *Inorg. Chem.* **1985**, *24*, 3381−3387.
(38) Muller, J. G. Grzybowski, J. J. Takeuchi, K. J. *Inorg. Chem.* **1986**, *25*, 2665−2667.
(39) Jackels, S. C.; Rose, N. J. *Inorg. Chem.* **1973**, *12*, 1232−1237.

Table 1. Selected Crystallographic Data of $[Mn(CDOH)_2(CDO)-(BBu(OC_2H_5))_2]$ and $[Mn(CDOH)_3BPh]OH\cdot CHCl_3$

	$[Mn(CDOH)_2(CDO)-(BBu(OC_2H_5))_2]$	$[Mn(CDOH)_3BPh]OH\cdot CHCl_3$
formula	$C_{30}H_{52}B_2MnN_6O_8$	$C_{25}H_{34}BCl_3MnN_6O_7$
fw	701.34	702.69
space group	$P2_1/n$ (No. 14)	*Pbca* (No. 61)
a (Å)	17.8789(6)	12.6712(5)
b (Å)	10.3613(4)	18.2899(4)
c (Å)	20.9762(8)	26.8276(9)
β (deg)	112.2941(19)	
V (Å^3)	3595.3(2)	6217.4(3)
Z	4	
d_{calcd} (g cm^3)	1.296	1.501
T (K)	150	150
crystal dimensions (mm^3)	0.48 × 0.45 × 0.38	0.30 × 0.28 × 0.13
Mo Kα λ (Å)	0.71073	0.71073
linear absorption coefficient (mm^{-1})	0.403	0.718
transmission factors	0.80−0.86	0.863−0.914
$R(F_o)^a$	0.065	0.048
$R_w(F_o^2)^b$	0.169	0.123

^{a} $R = \sum||F_o| - |F_c||/\sum|F_o|$ for $F_o^2 > 2\sigma(F_o^2)$. ^{b} $R_w = [\sum w(|F_o^2| - |F_c^2|)^2/\sum w|F_o^2|^2]^{1/2}$.

Table 2. Selected Bond Distances (Å) of $[Mn(CDOH)_2(CDO)(BBu(OC_2H_5))_2]$ and $[Mn(CDOH)_3BPh]OH\cdot CHCl_3$

$[Mn(CDOH)_2(CDO)(BBu(OC_2H_5))_2]$			$[Mn(CDOH)_3BPh]OH\cdot CHCl_3$		
atom 1	atom 2	distance (Å)	atom 1	atom 2	distance (Å)
Mn	N(11)	2.308(3)	Mn	N(11)	2.242(3)
Mn	N(12)	2.275(3)	Mn	N(12)	2.260(3)
Mn	N(21)	2.278(3)	Mn	N(21)	2.262(3)
Mn	N(22)	2.237(2)	Mn	N(22)	2.232(3)
Mn	N(31)	2.313(2)	Mn	N(31)	2.213(3)
Mn	N(32)	2.246(2)	Mn	N(32)	2.272(3)
O(11)	N(11)	1.376(3)	O(11)	N(11)	1.383(3)
O(12)	N(12)	1.381(3)	O(12)	N(12)	1.372(3)
O(21)	N(21)	1.378(3)	O(21)	N(21)	1.386(3)
O(22)	N(22)	1.381(3)	O(22)	N(22)	1.381(3)
O(31)	N(31)	1.375(3)	O(31)	N(31)	1.387(3)
O(32)	N(32)	1.382(3)	O(32)	N(32)	1.376(3)
O(11)	B(1)	1.493(5)	O(11)	B(1)	1.490(4)
O(21)	B(1)	1.499(5)	O(21)	B(1)	1.499(4)
O(111)	B(1)	1.460(5)	O(31)	B(1)	1.505(4)
O(22)	B(2)	1.492(4)	O(12)	H(12)	0.87(3)
O(31)	B(2)	1.493(4)	O(22)	H(22)	0.87(3)
O(211)	B(2)	1.472(4)	O(32)	H(32)	0.86(3)

(s, υ_{N-O}); 1172 and 810 (s, υ_{B-O}). ESI-MS *m*/*z*: (positive mode) 426 (calcd for $[MnC_{13}H_{23}N_6O_6B]^+$, 426.12).

$[Mn(CDOH)_3BPh]OH$. Crystals of $[Mn(CDOH)_3BPh]OH\cdot CHCl_3$ suitable for X-ray crystallographic analysis were obtained from slow evaporation of the chloroform solution containing $[Mn(CDO)_3(BPh)_2]$. IR (KBr, cm^{-1}): 3434 (s, υ_{O-H}); 1605, 1513, 1453, 1419, 1340 (s, $\upsilon_{C=N}$ and υ_{ring}); 1211, 1043 (s, υ_{N-O}); 1172 and 810 (s, υ_{B-O}). ESI-MS *m*/*z*: (positive mode) 566 (calcd for $[MnC_{24}H_{32}N_6O_6B]^+$, 566.19).

Solution Stability Experiments. The Mn(II) complex (1 mg) was dissolved in 2 mL of a mixture of methanol and acetonitrile (50:50 v/v). Samples from the resulting solution were analyzed by HPLC (λ = 265 nm) at t = 0, 1, 3, 5, and 8 h post-dissolution. The chelator challenge experiment was performed by dissolving the Mn(II) complex (1 mg) in 2 mL of a mixture of water and acetonitrile (50:50 v/v). PDTA was added in large excess (~100 fold), and the pH was 7.5. Samples from the mixture were analyzed by HPLC at t = 0, 1, 3, 5, and 8 h post-dissolution.

X-ray Crystallographic Analysis. Selected crystallographic data for complexes $[Mn(CDOH)_3BPh]OH\cdot CHCl_3$ and $[Mn(CDOH)_2(CDO)(BBu(OC_2H_5))_2]$ were collected on a Nonius Kappa CCD diffractometer and are listed in Table 1. The selected bond distance and bond angles are listed in Tables 2 and 3, respectively. Crystals were mounted on a glass fiber in a random orientation. Preliminary examination and data collection were performed using graphite-monochromated Mo Kα radiation (λ = 0.71073 Å). Cell constants and an orientation matrix for data collection were obtained from least-squares refinement, using setting angles in the range of $2° < \theta < 27°$ for $[Mn(CDOH)_2(CDO)(BBu(OC_2H_5))_2]$ and $1° < \theta < 24°$ for $[Mn(CDOH)_3BPh]OH\cdot CHCl_3$. A total of 24 681 reflections were collected and 5451 reflections were unique for $[Mn(CDOH)_3BPh]OH\cdot CHCl_3$. A total of 29 952 reflections were collected and 8440 reflections were unique for $[Mn(CDOH)_2(CDO)(BBu(OC_2H_5))_2]$. Lorentz and polarization corrections were applied to the data. A linear absorption coefficient is 4.0 cm^{-1} for Mo Kα radiation in $[Mn(CDOH)_2(CDO)(BBu(OC_2H_5))_2]$ and 7.2 cm^{-1} in $[Mn(CDOH)_3BPh]OH\cdot CHCl_3$. An empirical correction was applied using the program SCALEPACK.[40] Both structures were solved by the direct method using SIR2002[41] and refined on a Linux PC using SHELXL97.[42] Crystallographic drawings were produced using the program ORTEP.[43]

Table 3. Selected Bond Angles (deg) of $[Mn(CDOH)_2(CDO)(BBu(OC_2H_5))_2]$ and $[Mn(CDOH)_3BPh]OH\cdot CHCl_3$

$[Mn(CDOH)_2(CDO)(BBu(OC_2H_5))_2]$				$[Mn(CDOH)_3BPh]OH\cdot CHCl_3$			
atom 1	atom 2	atom 3	angle (deg)	atom 1	atom 2	atom 3	angle (deg)
N(11)	Mn	N(12)	68.82(9)	N(11)	Mn	N(12)	70.36(10)
N(21)	Mn	N(22)	70.42(9)	N(21)	Mn	N(22)	70.80(9)
N(31)	Mn	N(32)	69.82(8)	N(31)	Mn	N(32)	70.61(9)
N(12)	Mn	N(22)	114.40(9)	N(12)	Mn	N(22)	102.74(10)
N(12)	Mn	N(32)	94.18(9)	N(12)	Mn	N(32)	99.43(10)
N(22)	Mn	N(32)	133.94(10)	N(22)	Mn	N(32)	100.98(9)
N(11)	Mn	N(21)	79.36(10)	N(11)	Mn	N(21)	78.03(9)
N(11)	Mn	N(32)	82.34(10)	N(11)	Mn	N(31)	77.87(9)
N(21)	Mn	N(32)	116.65(9)	N(21)	Mn	N(31)	77.14(9)

Table 4. Elemental Analysis Data for Bis- and Monocapped Mn(II) Complexes

compd	C anal. (found)	H anal. (found)	N anal. (found)
$[Mn(CDO)_3(BPh)_2]\cdot 2H_2O$	52.40 (52.01)	5.53 (5.35)	12.22 (12.30)
$[Mn(CDOH)_3BPh]OH$	49.40 (49.75)	5.66 (5.47)	14.40 (14.02)
$[Mn(CDOH)_3BPh]Cl\cdot 0.75H_2O\cdot 0.5C_2H_5OH$	47.04 (47.17)	5.76 (5.54)	13.17 (12.89)
$[Mn(CDOH)_2(CDO)(BBu(OC_2H_5))_2]$	51.23 (50.98)	7.74 (7.52)	11.95 (11.92)
$[Mn(CDOH)_3BBu]Cl\cdot 1.75H_2O$	39.95 (39.75)	5.91 (5.49)	14.71 (14.77)
$[Mn(CDO)_3(BCH_3)_2]$	45.58 (45.23)	5.74 (6.06)	15.94 (15.57)
$[Mn(CDOH)_3BCH_3]Cl\cdot H_2O$	40.89 (40.73)	5.38 (5.46)	15.07 (14.94)
$[Mn(DMG)_3(BPh)_2]$	50.30 (50.27)	4.92 (4.76)	14.66 (14.56)
$[Mn(DMGH)_3BPh]OAc\cdot H_2O$	42.50 (42.15)	5.53 (5.64)	14.87 (14.58)
$[Mn(DMG)_3(BBu)_2]\cdot 0.5CH_3OH$	44.84 (45.01)	6.97 (7.12)	15.30 (14.95)
$[Mn(DMGH)_3BBu]OAc\cdot 0.5CH_3OH$	40.90 (41.12)	6.49 (6.55)	15.47 (15.31)
$[Mn(DMG)_3(BCH_3)_2]\cdot H_2O$	36.72 (36.43)	5.50 (5.55)	18.35 (18.22)
$[Mn(DMGH)_3BCH_3]OAc\cdot 0.5CH_3OH$	37.11 (37.15)	5.93 (6.02)	16.75 (16.56)

Scheme 1. Synthesis of Biscapped and Monocapped Mn(II) Complexes

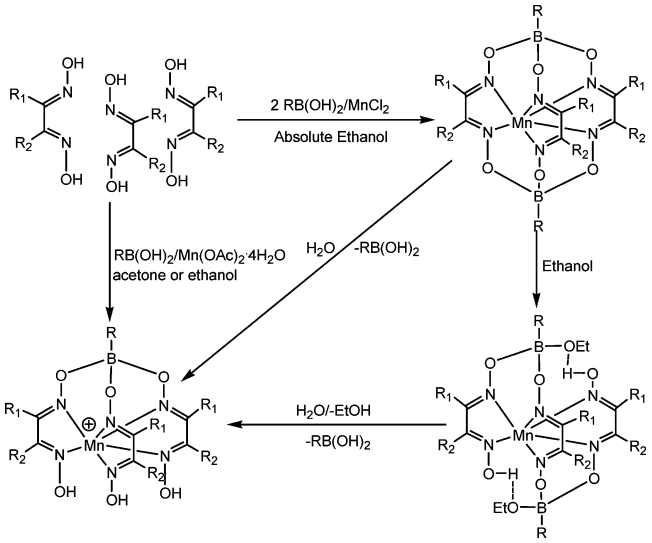

Results and Discussion

Synthesis of Biscapped and Monocapped Mn(II) Complexes. Biscapped Mn(II) complexes $[Mn(dioxime)_3(BR)_2]$ (Figure 1, complex A; dioxime = $CDOH_2$ and $DMGH_2$; R = Me, *n*-Bu, and Ph) were prepared according to Scheme 1 by reacting anhydrous Mn(II) chloride with 3 equiv of dioximes and 2 equiv of alkyl- or arylboronic acids in absolute ethanol under a nitrogen atmosphere. Complexes $[Mn(dioxime)_3(BR)_2]$ are stable in the solid state but decompose rapidly in the presence of water. $[Mn(CDOH)_2(CDO)(BBu(OC_2H_5))_2]$ was isolated from the ethanol solution containing $[Mn(CDO)_3(BBu)_2]$ during recrystallization. Cationic complexes $[M(dioxime)_3BR]^+$ (Figure 1, complex D; dioxime = CDOH and DMGH; R = Me, *n*-Bu, and Ph) were prepared in a similar fashion except that only 1 equiv of alkyl- or arylboronic acid was used. The addition of alkyl- or arylboronic acid had to be slow to minimize formation of the corresponding biscapped Mn(II) complex. Cationic complexes $[M(dioxime)_3BR]^+$ could also be prepared by hydrolysis of biscapped complexes $[Mn(dioxime)_3(BR)_2]$ in a mixture of water and acetonitrile or chloroform with a trace amount of water. For example, crystals of the complex $[Mn(CDOH)_3BPh]OH\cdot CHCl_3$ suitable for X-ray crystallographic analysis were isolated from the chloroform solution containing $[Mn(CDO)_3(BPh)_2]$ in the presence of air. Both the biscapped and monocapped Mn(II) complexes have been characterized by elemental analysis (Table 4), IR, UV/vis, ESI-MS, cyclic voltammetry (Table 5), and, in the cases of $[Mn(CDOH)_3BPh]OH\cdot CHCl_3$ and $[Mn(CDOH)_2(CDO)(BBu(OC_2H_5))_2]$, X-ray crystallography.

Table 5. Summary of Oxidation Potentials (E_{ox}) and Extinction Coefficients (ϵ) for Biscapped and Monocapped Mn(II) Complexes

compd	E_{ox} (V)[a]	ϵ (M^{-1} cm^{-1})*
$[Mn(CDO)_3(BPh)_2]$	1.35	16 250
$[Mn(CDOH)_3BPh]Cl$	1.35	16 250
$[Mn(CDOH)_2(CDO)(BBu(OC_2H_5))_2]$	1.31	15 550
$[Mn(CDOH)_3BBu]Cl$	1.31	15 550
$[Mn(CDO)_3(BCH_3)_2]$	1.26	14 350
$[Mn(CDOH)_3BCH_3]Cl$	1.26	14 350
$[Mn(DMG)_3(BPh)_2]$	1.25	14 750
$[Mn(DMGH)_3BPh]OAc$	1.25	14 750
$[Mn(DMG)_3(BBu)_2]$	1.22	13 950
$[Mn(DMGH)_3BBu]OAc$	1.22	13 950
$[Mn(DMG)_3(BCH_3)_2]$	1.20	12 950
$[Mn(DMGH)_3BCH_3]OAc$	1.20	12 950

[a] Both cyclic voltammograms and extinction coefficients of Mn(II) complexes were obtained in acetonitrile containing a trace amount of water (0.02%).

Spectroscopic Characterization. The IR spectra of both the monocapped and biscapped complexes are similar to those reported for $[M(dioxime)_3(BR)_2]$ (M = Fe, Co, and Ru) and $[MX(dioxime)_3BR]$ (M = Tc and Re; X = Cl, Br, NCS, and SCN; R = alkyl and aryl).[26,27,38,39] The single band between 1650 and 1550 cm^{-1} is due to the C=N stretch. Several strong bands between 950 and 1050 cm^{-1} and 1220−1270 cm^{-1} are tentatively assigned as N−O stretches, and the multiple absorption bands at 810−815 cm^{-1} and 1000−1200 cm^{-1} are due to the B−O stretches. The UV/visible spectra of both monocapped and biscapped Mn(II) complexes in chloroform show no transitions in the visible region (400−800 nm) because of the high-spin d^5 configuration of Mn(II). The single transition that has been observed in the UV region is in the range of 250−270 nm with an extinction coefficient value around 12 000−17 000 (Table 5). This transition is likely due to the metal-to-ligand charge transfer (MLCT).

(40) Otwinowski, Z.; Minor, W. *Methods Enzymol.* **1997**, *276*, 307−326.
(41) Burla, M. C.; Camalli, M.; Carrozzini, B.; Cascarano, G. L.; Giacovazzo, C.; Polidori, G.; Spagna, R. *J Appl. Crystallogr.* **2003**, *36*, 1103.
(42) Shelderick, G. M. *SHELXL 97: A Program for Crystal Structure Refinement*; University of Göttingen: Göttingen, Germany, 1997.
(43) Johnson, C. K. *ORTEPII*; Report ORNL-5138; Oak Ridge National Laboratory: Oak Ridge, TN, 1976.

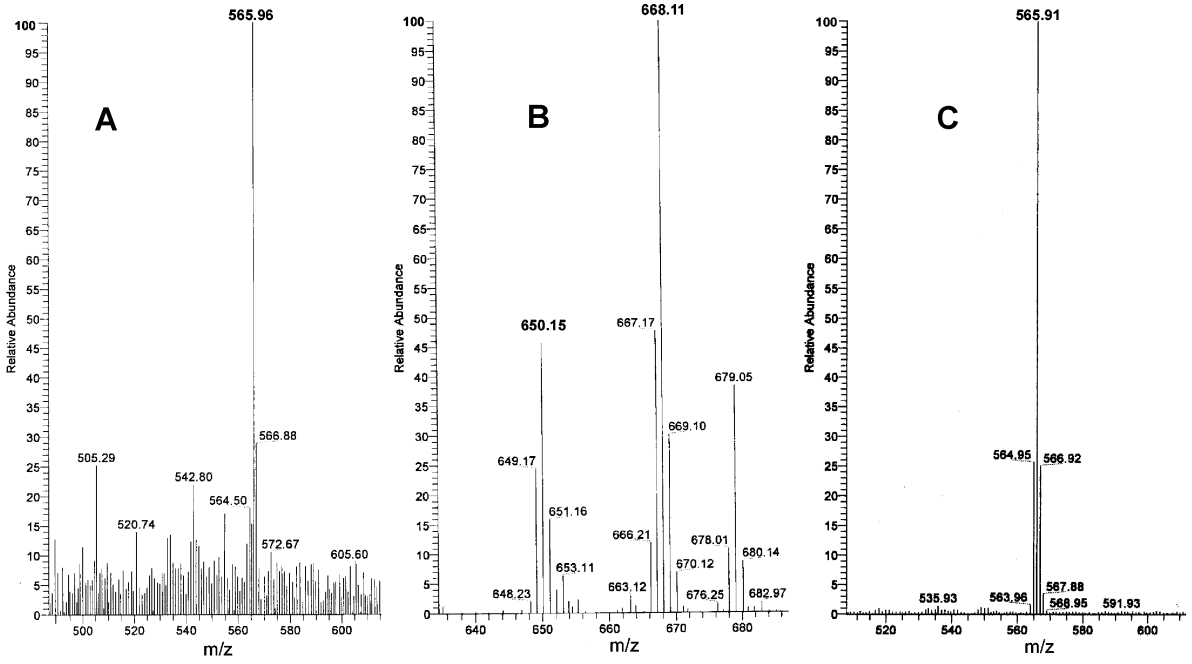

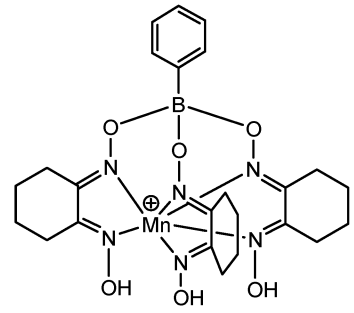

$C_{24}H_{32}BMnN_6O_6^+$: m/e = 566.19 (100.0%), 567.19 (26.0%) and 565.19 (23.2%)

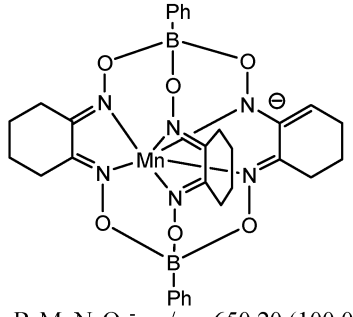

$C_{30}H_{33}B_2MnN_6O_6^-$: m/e = 650.20 (100.0%), 649.21 (51.3%), and 651.21 (37.4%)

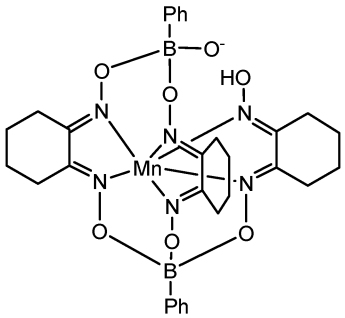

$C_{30}H_{35}B_2MnN_6O_7^-$: m/e = 668.21 (100.0%), 667.22 (51.3%), and 669.22 (37.6%)

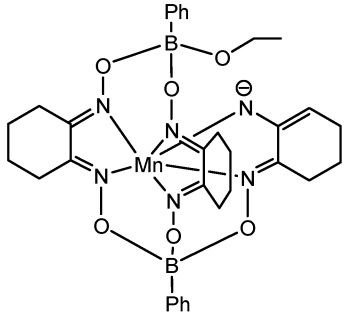

$C_{32}H_{38}B_2MnN_6O_6^-$: m/e = 679.24 (100.0%), 678.25 (51.5%) and 680.25 (40.1%)

Figure 2. ESI-MS spectra of $[Mn(CDO)_3(BPh)_2]$ in positive mode (A) and negative mode (B), and that of $[Mn(CDOH)_3BPh]^+$ in positive mode (C), along with the proposed molecular fragments. The ethoxy group might come from crystallization ethanol in the bulk sample.

ESI-MS data of biscapped and monocapped Mn(II) complexes were obtained using chloroform, acetonitrile, or methanol as the matrix, depending on the complex solubility. Figure 4 shows typical ESI-MS spectra of $[Mn(CDO)_3(BPh)_2]$ and $[Mn(CDOH)_3BPh]^+$ using chloroform as the matrix. The positive mode ESI-MS spectra of both biscapped and monocapped Mn(II) complexes show the molecular ion $[Mn(dioxime)_3BR]^+$ (panels A and B of Figure 2). The negative mode ESI-MS spectrum of $[Mn(CDO)_3(BPh)_2]$ shows the expected molecular ion, $[M-H]^-$, and the hydrolyzed molecular ion $[M + H_2O - H]^-$ (Figure 2B), which are not observed in the negative mode ESI-MS spectrum of $[Mn(CDOH)_3BPh]^+$. This suggests that complexes $[Mn(dioxime)_3(BR)_2]$ are indeed synthesized, even though they are unstable in aqueous solution. However, this cannot completely exclude the presence of the partially capped complex (Figure 2). The positive mode ESI-MS spectrum of $[Mn(CDOH)_2(CDO)(BBu(OC_2H_5))_2]$ always

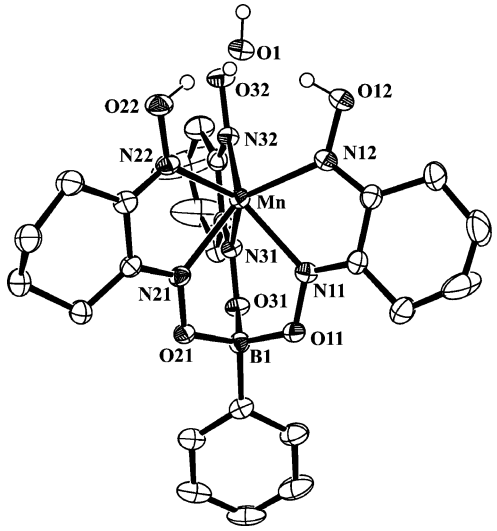

Figure 3. ORTEP diagram of [Mn(CDOH)$_3$BPh](OH). (Ellipsoids are at the 50% probability level). Crystallization chloroform and hydrogen atoms are omitted for the sake of clarity.

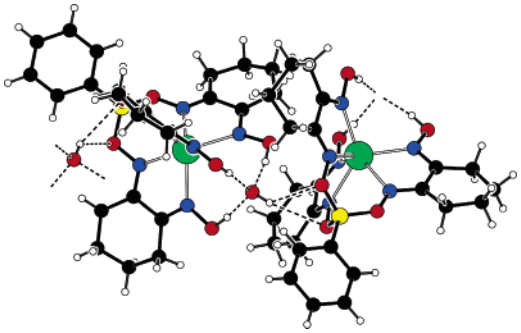

Figure 4. H-bonding network in [Mn(CDOH)$_3$BPh]OH.

shows the molecular ion due to [Mn(CDOH)$_3$BBu]$^+$. It loses one boron cap and one ethanol from the remaining boron cap in the mass spectrophotometer. These findings are completely consistent with the instability of biscapped Mn(II) complexes in protic solvents.

X-ray Crystal Structure of [Mn(CDOH)$_3$BPh]OH·CHCl$_3$. The ORTEP drawing of [Mn(CDOH)$_3$BPh]OH is illustrated in Figure 3. Figure 4 shows the H-bonding network in [Mn(CDOH)$_3$BPh]OH. Crystallization chloroform and hydrogen atoms are omitted for the sake of clarity. There are four [Mn(CDOH)$_3$BPh]$^+$ cations in each unit cell. In general, [Mn(CDOH)$_3$BPh]$^+$ has a near C_3 symmetry. The Mn(II) is coordinated with six nitrogen atoms from three dioxime chelating arms, which are capped by a tetrahedral boron atom at one end through three covalent B−O bonds. The coordination geometry is best described as trigonal prismatic, with the two triangular planes being defined by N11−N21−N31 and N12−N22−N32. These two triangular planes are almost parallel, with the dihedral angle at 1.4(2)°. The average Mn−N distance in [Mn(CDOH)$_3$BPh]OH is 2.247(3) Å, which is well comparable to those observed in the Mn(II) complexes with distorted trigonal prismatic coordination geometry.[44−46] The average Mn−N bond length at the boron-capped end is about 0.016(3) Å shorter than that at the uncapped end because of constraints imposed by the boron cap. This difference is smaller than that found in the monocapped tris(dioxime) Tc(III) and Re(III) complexes, probably because of their differences in size and coordination number of the metal ion.[28,29] Each dioxime chelating arm forms a planar five-membered chelate ring with the Mn(II) center. The average bidentate bite angle is 70.59(9)°, which is smaller than those observed in other biscapped and monocapped tris(dioxime) metal complexes,[27−29] most likely because of the large size of Mn(II). Three hydroxyl groups from the dioxime chelating arms in [Mn(CDOH)$_3$BPh]OH form strong intramolecular hydrogen bonds with the hydroxide counterion. The average hydrogen bond distance is 0.87 Å. These hydrogen bonds in some way act as a topological closure (B−Mn−O angle = 179.45°). Therefore, the structure of [Mn(CDOH)$_3$BPh]OH can be considered as being the clathrochelate type with the hydroxide counterion as a cap. In addition, there are two strong intermolecular hydrogen bonds between the hydroxide hydrogen and two oxygen atoms of the three B−O bonds (Figure 4).

The structure of [Mn(CDOH)$_3$BPh]OH is different from those of the tris(dioxime) complexes, [MCl(dioxime)$_3$BR] (M = Tc and Re; R = alkyl and aryl),[26−31] in which Tc and Re are seven-coordinated and the two uncapped dioxime (CDOH) groups form strong intramolecular hydrogen bonds with the deprotonated CDO (Figure 1, complex B).[26−29] It is surprising to see that the Mn(II) in [Mn(dioxime)$_3$BR]$^+$ is six-coordinated, whereas smaller metal ions, Tc(III) and Re(III), in [MCl(dioxime)$_3$BR] are seven-coordinated by virtually the same monocapped tris(dioxime) chelating system. We believe that this structural difference is probably related to the charge of metal ions. For cationic complexes [Mn(dioxime)$_3$BR]$^+$, the Mn(II) is highly stabilized by six imine-N donors, and the intramolecular hydrogen bonding between the hydroxide counterion (Figure 4) and hydroxyl groups of the CDOH chelating arms prevents the coordination of other ligands, such as chloride, to the Mn(II). In complexes [MCl(dioxime)$_3$BR] (M = Tc and Re), the metal ion is in the +3 oxidation state. The monodentate ligand and the intramolecular hydrogen bonding are needed to satisfy their neutrality.

It is interesting to note that the biscapped complexes [M(dioxime)$_3$(BR)$_2$] (M = Fe and Co) are stable, whereas the biscapped tris(dioxime) Mn(II) complexes [Mn(dioxime)$_3$(BR)$_2$] tend to hydrolyze in the presence of water. This is probably related to the size of the metal ions. For complexes [M(dioxime)$_3$(BR)$_2$] (M = Fe and Co),[38,39] the metal ions are relatively small (ionic radii = 0.61 and 0.65 Å for Co(II) and Fe(II),[47] respectively) and fit into the coordination cavity of the biscapped tris(dioxime) ligand. For [Mn(dioxime)$_3$(BR)$_2$], however, Mn(II) (ionic radius = 0.67 Å) is larger than Co(II) and Fe(II).[47] Its size may not match the cavity of the tris(dioxime) ligand and causes significant constraints to the ligand framework. Losing one of the two boron caps allows the tris(dioxime) ligand to release these constraints

(44) Mikuriya, M.; Fukumoto, H.; Kako, T. *Inorg. Chem. Commun.* **1998**, *1*, 225−227.
(45) Mikuriya, M.; Hatano, Y.; Asato, E. *Bull. Chem. Soc. Jpn.* **1997**, *70*, 2495−2507.
(46) Mikuriya, M.; Hatano, Y.; Asato, E. *Chem. Lett.* **1996**, 849−850.
(47) Shannon, R. D. *Acta Crystallogr., Sect. A* **1976**, *32*, 751−767.

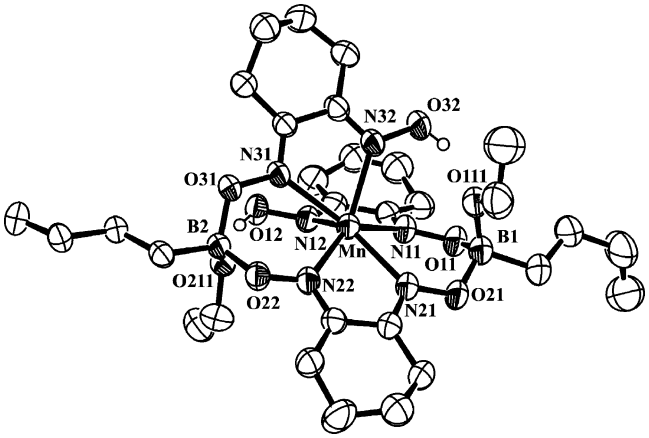

Figure 5. ORTEP diagram of $[Mn(CDOH)_2(CDO)(BBu(OC_2H_5))_2]$. (Ellipsoids are at the 50% probability level). Hydrogen atoms are omitted for the sake of clarity.

while remaining able to completely wrap Mn(II) with its six imine-N donor atoms. That may explain why biscapped Mn(II) complexes $[Mn(dioxime)_3(BR)_2]$ tend to hydrolyze in the presence of water, whereas the biscapped metal complexes $[M(dioxime)_3(BR)_2]$ (M = Fe and Co) remain stable.

X-ray Crystal Structure of $[Mn(CDOH)_2(CDO)(BBu(OC_2H_5))_2]$. Figure 5 shows the ORTEP drawing of $[Mn(CDOH)_2(CDO)(BBu(OC_2H_5))_2]$, which is almost identical to that of $[Mn(CDOH)_2(CDO)(BPh(OCH_3))_2]$.[29] Mn(II) is coordinated by six imine-N atoms, and the coordination geometry is distorted trigonal prism. One triangular plane is defined by N11, N21, and N32, whereas the other is defined by N12, N22, and N31. The dihedral angle between these two triangular planes is 3.21(13)°. The average Mn−N distance is 2.276(3) Å, consistent with the Mn−N (dioxime) distances reported by Jurisson and co-workers.[29] Each dioxime group forms a planar five-membered chelate ring with Mn(II). The average bite angle is 69.69(9)°.

In $[Mn(CDOH)_2(CDO)(BBu(OC_2H_5))_2]$, only one of three dioxime chelating arms is bonded to both boron atoms. The other two are bonded to one boron atom at one end and have a hydroxyl group at the other end. Both boron atoms are bonded to three oxygen atoms: two from the hydroxyl groups of two dioxime chelating arms and the third from the ethoxyl group. In this way, the constraints imposed by the mismatch between Mn(II) and coordination cavity of the tris(CDOH) ligand can be released while it is still able to wrap the Mn(II) with its six imine-N donor atoms. That may explain why $[Mn(CDOH)_2(CDO)(BBu(OC_2H_5))_2]$ is isolated during recrystallization of $[Mn(CDOH)_3(BBu)_2]$ from ethanol.

Solution Instability of Biscapped Mn(II) Complexes. We used a reversed-phase HPLC method to monitor the solution stability of Mn(II) complexes. It was found that both $[Mn(CDO)_3(BPh)_2]$ and $[Mn(CDOH)_3BPh]OH$ have the same retention time at ∼16 min. To confirm this observation, we co-injected $[Mn(CDO)_3(BPh)_2]$ and $[Mn(CDOH)_3BPh]$-OH using the same HPLC method. Figure 6 shows a representative HPLC chromatogram of the aqueous solution containing $[Mn(CDO)_3(BPh)_2]$ and $[Mn(CDOH)_3BPh]OH$. The 16 min peak was the only signal detected, suggesting that the compounds share the same composition in the HPLC mobile phase. The ESI-MS spectrum of the collected fraction at ∼16 min displayed a molecular ion at $m/z = 566$ that corresponds to $[Mn(CDOH)_3BPh]^+$, clearly demonstrating that $[Mn(CDO)_3(BPh)_2]$ is not stable in aqueous solution. As soon as $[Mn(CDO)_3(BPh)_2]$ is in contact with water in the HPLC mobile phase, one of the boron caps quickly hydrolyzes to form $[Mn(CDOH)_3BPh]OH$. These results would explain why crystals of $[Mn(CDOH)_3BPh]OH$ were isolated from the slow evaporation of the chloroform solution containing $[Mn(CDO)_3(BPh)_2]$. Similar instability was observed for $[Mn(CDOH)_2(CDO)(BBu(OC_2H_5))_2]$ in aqueous solution.

Solution Stability of Monocapped Mn(II) Complexes. The results from the stability experiment also showed that $[Mn(CDOH)_3BPh]OH$ remained stable in solution for more than 8 h. To further demonstrate its solution stability, we carried out a chelator challenge experiment in a mixture of acetonitrile and water (50:50 v/v) with a large excess of added PDTA (∼100-fold), which forms stable Mn(II) complex $Mn(PDTA)^{-2}$ with a log K value of 15.[48] It was found that the peak intensity at ∼16 min from $[Mn(CDOH)_3BPh]^+$ remains unchanged over 8 h (Figure 7) and that the pH (5.0−9.0) has no significant impact on the stability of $[Mn(CDOH)_3BPh]^+$. These data clearly dem-

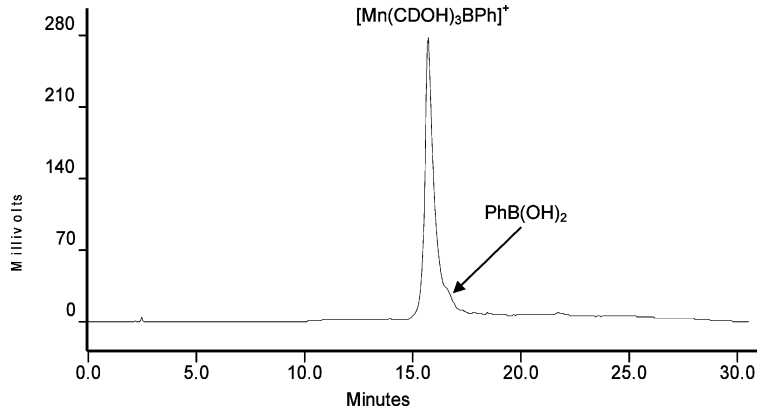

Figure 6. Typical HPLC chromatogram of the solution containing $[Mn(CDO)_3(BPh)_2]$ and $[Mn(CDOH)_3BPh]OH$. The presence of a $PhB(OH)_2$ peak at ∼16.5 min is caused by the hydrolysis of $[Mn(CDO)_3(BPh)_2]$.

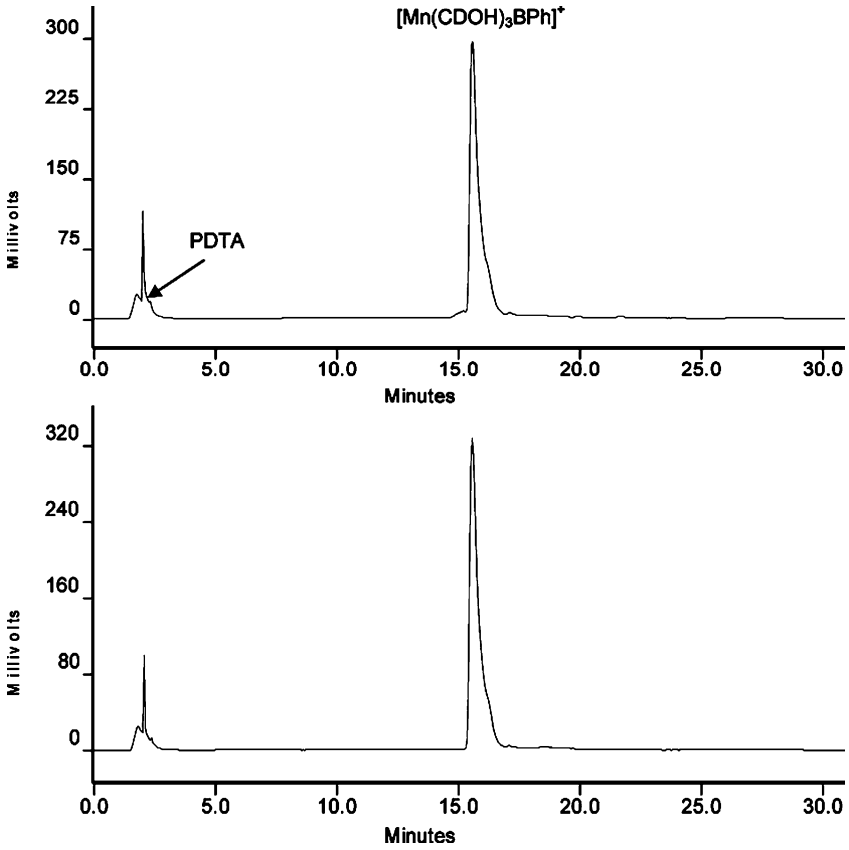

Figure 7. HPLC chromatograms of the aqueous solution of $[Mn(CDOH)_3BPh]Cl$ at 0.5 h (top) and 8 h (bottom) after the addition of a 100-fold excess of PDTA.

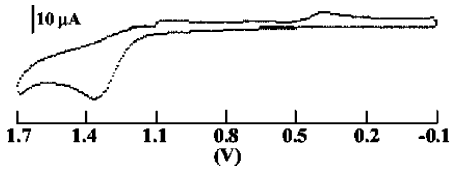

Figure 8. Typical cyclic voltammogram of $[Mn(CDOH)_3BPh]Cl$. The concentrations of Mn(II) complexes were about 2 mM in acetonitrile. The oxidation potential is given as that vs NHE, because the $Ag/AgNO_3$ electrode has a potential of +0.4 V vs NHE. The scan rate was 100 mV/s.

onstrated the solution stability of cationic complexes $[Mn(dioxime)_3BR]^+$. It is important to note that most Mn(II) complexes are not thermodynamically stable because of a lack of ligand-field stabilization energy.[49] In $[Mn(CDOH)_3BPh]^+$, the Mn(II) is completely wrapped by six imine-N donor atoms so that it is very difficult for Mn(II) to become dissociated. Therefore, the high solution stability of cationic complex $[Mn(CDOH)_3BPh]^+$ is most likely due to its kinetic inertness imposed by the boron-capped tris(CDOH) chelator.

Electrochemistry. Cyclic voltammograms were obtained using acetonitrile as the solvent for both biscapped and monocapped Mn(II) complexes. They all show an irreversible one-electron oxidation wave at 1.20−1.35 V vs NHE, depending on the identity of the boron cap and dioxime chelating arms. Figure 8 shows a cyclic voltammogram of $[Mn(CDO)_3BPh]Cl$. The oxidation potentials of biscapped and monocapped Mn(II) complexes are summarized in Table 5. The fact that biscapped Mn(II) complexes $[Mn(dioxime)_3(BR)_2]$ have oxidation potentials identical to those of their cationic analogues provides further support for our conclusion that they are not stable and form cationic complexes $[M(dioxime)_3BR]^+$ in the presence of water. As the boron cap becomes smaller (phenyl, *n*-butyl, and methyl), the oxidation potential of $[M(dioxime)_3BR]^+$ decreases. A similar trend was also observed when CDOH was replaced by DMGH in cationic complexes $[M(dioxime)_3BR]^+$. The high oxidation potential for the Mn(II)/Mn(III) couple clearly indicates that the +2 oxidation state is highly stabilized by six soft imine-N donors. The irreversibility suggests that the oxidation from Mn(II) to Mn(III) probably involves significant conformational changes of the coordinated dioxime ligand. Similar irreversibility was also observed in the monocapped Fe(II) clathrochelates.[50,51]

Conclusion

The key finding of this study is that the biscapped complexes $[Mn(dioxime)_3(BR)_2]$ can be readily prepared, even though they are not stable in the presence of water. One of the boron caps quickly hydrolyzes to for cationic complexes $[M(dioxime)_3BR]^+$, which are stable in aqueous solution in the presence of a strong Mn(II) chelator such as PDTA. This high solution stability is most likely due to the

(48) Ogino, H. *Bull. Chem. Soc. Jpn.* **1965**, *38*, 771−778.
(49) Ijeri, V. S.; Srivastava, A. K. *Polyhedron* **2003**, *22*, 569−574.
(50) Bieda, K. L.; Kranitz, A. L.; Grzybowski, J. J. *Inorg. Chem.* **1993**, *32*, 4209−4213.
(51) Belinski, J. A.; Squires, M. E.; Kuchna, J. M.; Bennett, B. A.; Grzybowski, J. J. *J. Coord. Chem.* **1988**, *19*, 159−169.

kinetic inertness imposed by the boron capped tris(dioxime) chelators that are able to completely wrap the Mn(II) into their N_6 coordination cavity. The three hydroxyl groups from dioxime chelating arms in $[Mn(CDOH)_3BPh]OH$ form strong intramolecular hydrogen bonds with the hydroxide counterion. Therefore, its structure can be considered as being clathrochelate with a hydroxide as a cap.

Acknowledgment. Acknowledgment is made to Dr. Phillip E. Fanwick, Department of Chemistry, Purdue University, for X-ray diffraction analysis of $[Mn(CDOH)_3BPh]OH \cdot CHCl_3$ and $[Mn(CDOH)_2(CDO)(BBu(OC_2H_5))_2]$. This work is supported, in part, by Purdue University, Bristol-Myers Squibb Medical Imaging Inc., and the following research grants: AHA0555659Z (S.L.) from the Greater Midwest Affiliate of the American Heart Association, R21 EB003419 (S.L.) from the National Institute of Biomedical Imaging and Bioengineering (NIBIB), and BCTR0503947 (S.L.) from the Susan G. Komen Breast Cancer Foundation.

Supporting Information Available: X-ray crystallographic files in CIF format for the reported structures of $[Mn(CDOH)_3BPh]OH$ and $[Mn(CDOH)_2(CDO)(BBu(OC_2H_5))_2]$. This material is available free of charge at http://pubs.acs.org.

IC060216N